



## Molecular Crystals and Liquid Crystals

Publication details, including instructions for authors and subscription information:

<http://www.tandfonline.com/loi/gmcl20>

### Selective Calcium Oxalate Crystallization Induced by Monomethylitaconate Grafted Polymethylsiloxane

A. Neira-Carrillo<sup>a c</sup>, P. Vásquez-Quitral<sup>a</sup>, M. Yazdani-Pedram<sup>b c</sup> & J. L. Arias<sup>a c</sup>

<sup>a</sup> Faculty of Veterinary and Animal Sciences, University of Chile, Santiago, Chile

<sup>b</sup> Faculty of Science Chemistry and Pharmaceutics, University of Chile, Santiago, Chile

<sup>c</sup> Center for Advanced Interdisciplinary Research in Materials (CIMAT), Santiago, Chile

Version of record first published: 28 May 2010

To cite this article: A. Neira-Carrillo, P. Vásquez-Quitral, M. Yazdani-Pedram & J. L. Arias (2010): Selective Calcium Oxalate Crystallization Induced by Monomethylitaconate Grafted Polymethylsiloxane, *Molecular Crystals and Liquid Crystals*, 522:1, 7/[307]-17/[317]

To link to this article: <http://dx.doi.org/10.1080/15421401003722765>

PLEASE SCROLL DOWN FOR ARTICLE

Full terms and conditions of use: <http://www.tandfonline.com/page/terms-and-conditions>

This article may be used for research, teaching, and private study purposes. Any substantial or systematic reproduction, redistribution, reselling, loan, sub-licensing, systematic supply, or distribution in any form to anyone is expressly forbidden.

The publisher does not give any warranty express or implied or make any representation that the contents will be complete or accurate or up to date. The accuracy of any instructions, formulae, and drug doses should be independently verified with primary sources. The publisher shall not be liable for any loss, actions, claims, proceedings, demand, or costs or damages whatsoever or howsoever caused arising directly or indirectly in connection with or arising out of the use of this material.

# Selective Calcium Oxalate Crystallization Induced by Monomethylitaconate Grafted Polymethylsiloxane

A. NEIRA-CARRILLO,<sup>1,3</sup> P. VÁSQUEZ-QUITRAL,<sup>1</sup>  
M. YAZDANI-PEDRAM,<sup>2,3</sup> AND J. L. ARIAS<sup>1,3</sup>

<sup>1</sup>Faculty of Veterinary and Animal Sciences, University of Chile,  
Santiago, Chile

<sup>2</sup>Faculty of Science Chemistry and Pharmaceutics, University of Chile,  
Santiago, Chile

<sup>3</sup>Center for Advanced Interdisciplinary Research in Materials (CIMAT),  
Santiago, Chile

*Calcium oxalate (CaOx) is the main compound of human kidney stones, specifically calcium oxalate monohydrate crystals (COM). Normal human urine contains small crystals of calcium oxalate dihydrate (COD), which have reduced capacity to form stable aggregates and strong adhesion contacts to renal epithelial cell thus protecting kidney stone formation. Here, we report the preparation of a new monomethylitaconate grafted polymethylsiloxane, which was able to promote and stabilize COD crystals. Although the mechanisms involved in control of CaOx polymorphism still remain unclear, we believe that research using synthetic polymers would provide interesting chemical clues to develop calculi preventing-compounds.*

**Keywords** Biomineralization; calcium oxalate; human kidney stone; polymethylsiloxane

## Introduction

Kidney stone disease or nephrolithiasis is a complex encompassing several physico-chemical phenomena occurring sequentially or concurrently in human. Up to 15% of white males and 6% of all females will have at least one renal stone during their lifetime [1,2]. Molecules in healthy human urine including citrate, glycosaminoglycans (GAGs) and glycoproteins can block crystal adhesion to renal cells [3]. Citrate can be orally administered and it appears to be effective treatment against human kidney stones (HKS) formation. The potential mechanisms by which citrate prevents the HKS are e.g., increased urinary pH, decreased Tamm-Horsfall protein aggregation and decreased crystal adhesion to tubular cells [4]. However, not all patients tolerate oral citrate well whereas other remain active stone formers while receiving it. Although, the use of low-invasive operations employing shock wave lithotripsy and

---

Address correspondence to Dr. A. Neira-Carrillo, Faculty of Veterinary and Animal Sciences, University of Chile, Santiago, Chile. Tel.: (56-2)9785642; Fax: (56-2)9785526; E-mail: aneira@uchile.cl

endoscopic treatment have been a common treatment, the prevalence of urolithiasis has been increasing year by year. Many research has been carried out in the last decade to clarify the molecular mechanisms involved in the HKS formation by using CaOx crystals but still is not completely understood [5–12]. Many patients have metabolic abnormalities, such as over-excretion of calcium and oxalate ions in the urine, that seem to explain their tendency toward HKS formation [5]. The recurrence of HKS rate is quite high, about 50% at 10 years and 75% at 15 years when no treatment at all is given [6], dietary advice to reduce the risk seems to be important. Until now no pharmacological treatment is available for the prevention of HKS.

In nature, CaOx exists as three polymorphs: calcium oxalate monohydrate (COM), calcium oxalate dihydrate (COD) and calcium oxalate trihydrate (COT) [7]. CaOx is the most often crystalline phase in HKS. Oxalate is present in many foods and it has been reported an endogenous contribution closer to 50%, the remainder being of dietary origin [8]. Several investigations have shown that organic materials play an important role in the *in vitro* CaOx crystallization during the HKS process by using Langmuir monolayers [9,10], membrane vesicles [11] and phospholipids' micelles [12]. Proteins, phospholipids, polysaccharides and other polyanionic organic molecules are involved in the inhibition of CaOx nucleation, crystal growth and attachment to cells *in vitro*. Recently, it has been described that the *Sargassum fusiforme*, a sulfated polysaccharide isolated from the marine algae, could decrease the size of COM and COD crystals, inhibits the aggregation of COM and induces the formation of COD [13]. However, the mechanism how these biomolecules prevent the HKS is not completely understood.

On the other hand, polysiloxanes (PMS), usually referred to as silicones, find numerous applications in different fields of chemistry and engineering. PMS represents the most widely used silicon-containing polymer in different industrial and medical applications [14,15]. Polydimethylsiloxane (PDMS) and polyhydrogenmethylsiloxane (PHMS) have versatile properties such as flexibility, permeability to gases, low glass transition temperature, biocompatibility, etc. All these applications rely on the unique physical and chemical properties of silicones in the bulk form and at interfaces. Additionally, the hydrosilylation reaction of polymers have attracted great interest due to the practical outcome and recent development in silicon-based organic polymers [16,17]. The main synthetic route leading to the modification of polysiloxanes is the hydrosilylation of polysiloxanes containing labile Si–H bond and by using platinum catalysts [18]. Speier's catalyst is the most commonly used catalyst for these reactions [19]. Modified PMS polymers become very attractive as new templates for CaOx *in vitro* crystallization assays [20,21]. Although the production of modified PMS for both medical and non-medical application has been reported [22–26], the available information concerning the effect of PMS on pathological biomineralization of CaOx is very scarce. It is well known that PMS can be chemically modified by introducing chemical groups such as  $-\text{CO}_2\text{H}$ ,  $-\text{PO}_3\text{H}$ ,  $-\text{SO}_3\text{H}$ , which are found in biological macromolecules [27–29]. The presence of these functional groups in modified PMS can emulate the role of the biological molecules during the *in vivo* crystallization of CaOx. The present work is motivated by the possibility of using functionalized PMS as a template for *in vitro* CaOx crystallization and by the paucity published works with PMS in biomineralization field. We report here the synthesis of polymethylsiloxane grafted monomethylitaconate ( $\text{CO}_2\text{H}$ -PMS) and its effect on the nucleation and crystal growth of CaOx.

## Experimental

### Materials

Calcium chloride ( $\text{CaCl}_2$ ), sodium oxalate ( $\text{Na}_2\text{C}_2\text{O}_4$ ), ethanol, sodium hydroxide (Analytical grade) and tris(hydroxymethyl) aminomethane (TRIS), and toluene (99.9%) were obtained from Merck. Methylene chloride ( $\text{CH}_2\text{Cl}_2 \geq 99.5\%$ ) and Petroleum ethers 98% boiling range 40–60°C were from Sigma-Aldrich. These reagents were of the highest available grade. Distilled water was filtered through a filter membrane having a pore size of 0.2  $\mu\text{m}$ . Toluene and methylene chloride were dried and distilled under argon. Both were purified by refluxing over lithium aluminum hydride (Aldrich-95% pellets, particle size 10  $\times$  6 mm) for 72 h and Na, respectively. The dicyclopentadienyl platinum (II) chloride ( $\text{Cp}_2\text{PtCl}_2$ ) catalyst used for the hydrosilylation reaction was synthesized from hydrated hexachloroplatinic acid (IV) called Speier's catalyst and the dicyclopentadiene [30]. The monomethylitaconate (MMI) was synthesized by direct esterification of itaconic acid (Aldrich) with methanol and its purity was checked by  $^1\text{H}$  NMR spectroscopy as was described in a previous work [31]. The PDMS-co-PHMS ( $M_w$  of 16349 g/mol and polydispersity of  $D=2$ ) was synthesized through cationic ring opening polymerization from octamethylcyclsiloxane ( $\text{D}_4$ ) and 1,3,5,7-tetramethylcyclotetrasiloxane ( $\text{D}_4^{\text{H}}$ ). The PDMS-co-PHMS ( $\chi_{\text{D}_4}^{\circ} = 0.5$ ) was used for hydrosilylation reaction with purified MMI.

### Hydrosilylation Reaction

The hydrosilylation of PDMS-co-PHMS with MMI was carried out using  $\text{Cp}_2\text{PtCl}_2$  [32,33]. This catalyst is not commercially available. Briefly, MMI (20 mol-% excess respect to the Si–H of copolymer) was dissolved in 100 ml of sodium-dried, freshly distilled toluene together with the stoichiometric amount of PDMS-co-PHMS. The reaction mixture was heated to 85°C under argon and then 100  $\mu\text{l}$  of  $\text{Cp}_2\text{PtCl}_2$  in  $\text{CH}_2\text{Cl}_2$  was injected. The mole ratio of Pt/SiH catalyst was  $1.5 \times 10^{-4}$ . Then, the mixture was refluxed under argon with agitation until the FTIR showed that the hydrosilylation reaction was complete (ca. 24 h). The excess of solvent and the unreacted materials were removed with a Heidolph rotary evaporator at 70°C. The product was precipitated with petroleum benzene. The supernatant was separated and the resultant  $\text{CO}_2\text{H-PMS}$  was dried under vacuum at 50°C for 2 h. The yield from the hydrosilylation was 95%. The synthetic route for the preparation of  $\text{CO}_2\text{H-PMS}$  by hydrosilylation reactions is shown in Figure 1.

### In Vitro Crystallization of Calcium Oxalate

The crystallization of CaOx was carried out by using the method described by Yamaguchi [34]. The crystallizations were performed at pH 4, pH 6 or pH 9 and either at 25°C or 37°C. Briefly, 800  $\mu\text{l}$  of 2 mM  $\text{CaCl}_2$  in 0.2M buffer Bis-Tris at pH 4, pH 6 or pH 9 were placed in an Eppendorf tube. Followed by adding a 800  $\mu\text{l}$  of 2 mM sodium oxalate in 0.2M buffer Bis-Tris either at pH 4, pH 6 or pH 9. After that, the *in vitro* crystallizations of CaOx were carried out by using two different concentrations of PMS or  $\text{CO}_2\text{H-PMS}$ , either 32  $\mu\text{g/ml}$  or 1 mg/ml,

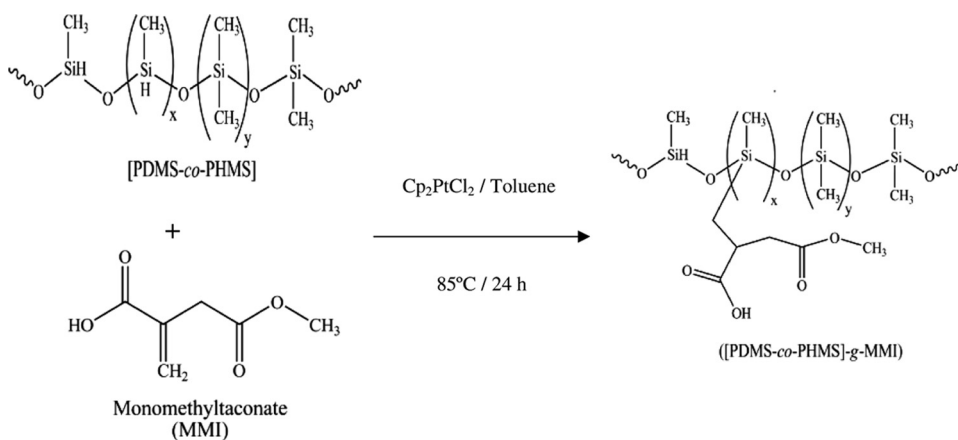


**Figure 1.** Synthesis of  $\text{CO}_2\text{H-PMS}$  by using hydrosilylation reaction.

at pH 4, pH 6 or pH 9, respectively. After 24 h the reaction mixture was filtered through  $0.2\ \mu\text{m}$  Millipore filter. The experimental set up for the crystallization of  $\text{CaOx}$  is shown in Figure 2. The resultant  $\text{CaOx}$  crystals were dried at room temperature for 24 h. Finally, small pieces of the Millipore filters containing  $\text{CaOx}$  crystals were fixed on a metallic support, coated with gold and observed by SEM.

### Measurements

Fourier transform infrared spectroscopy (FTIR) of  $\text{PDMS-co-PHMS}$  and  $\text{CO}_2\text{H-PMS}$  were obtained on a Bruker model Vector 22. The samples were prepared as potassium bromide pellets. The molecular weight (MW) determination of  $\text{PDMS-co-PHMS}$  was carried out by using PSS-Win GPC-PSS Gel Permeation Chromatography (GPC). The  $\text{CaOx}$  crystals formed after *in vitro* crystallization were

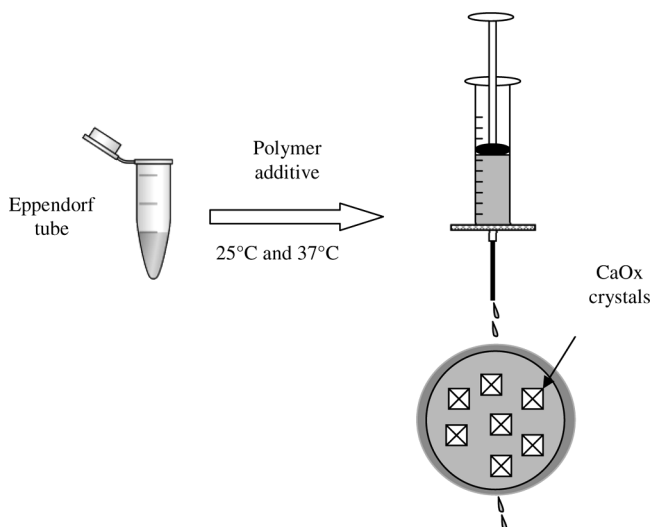


**Figure 2.** *In vitro* crystallization of  $\text{CaOx}$ .

dried, fixed to a metal support and then coated with gold using an automated sputter coater (EMS-550). Crystals of CaOx formed in the presence of PDMS-co-PHMS used as negative control and with CO<sub>2</sub>H-PMS were observed in a Tesla BS 343A scanning electron microscope at 15 kV. Additionally, TGA of PMS and CO<sub>2</sub>H-PMS were carried out in a Q50 V20.5 Build 30 instrument.

## Results and Discussion

The main synthetic route leading to the modification of PMS is the hydrosilylation reaction using platinum catalysts. The hydrosilylation refers to an addition of Si-H to C=C bonds and represents the usual synthetic route for laboratory scale preparation of organosilicon derivatives [26]. The hydrosilylation of the starting PDMS-co-PHMS was monitored by FTIR, following the decrease of the Si-H absorption band. Figure 3(A-C) represents the FTIR of PDMS-co-PHMS, MMI and CO<sub>2</sub>H-PMS. Figure 3A shows the FTIR spectrum of an organosilicon with typical absorption bands at 2967 cm<sup>-1</sup>, 2160 cm<sup>-1</sup>, 1105 cm<sup>-1</sup>, 1206 cm<sup>-1</sup> and 801 cm<sup>-1</sup> assigned to the stretching vibration of C-H, Si-H, Si-O-Si and Si-CH<sub>3</sub>, respectively [35,36]. The spectrum of MMI presented in Figure 3B shows the absorption bands due to the stretching vibration of C=O at 1729 cm<sup>-1</sup>. It is clearly seen from Figure 3C that the absorption band of Si-H from PDMS-co-PHMS disappeared demonstrating that the hydrosilylation reaction has took place. The absorption bands at 2961 cm<sup>-1</sup> represent the incorporation of carbon/hydrogen bonds on the main chain of CO<sub>2</sub>H-PMS. The presence of carboxylic and carbonyl groups and the silicon-oxygen ester bonds of the grafted CO<sub>2</sub>H-PMS corresponding to the stretching vibration of O-H, C=O and Si-O-Si bonds can be seen at 3502 cm<sup>-1</sup>, 1741 cm<sup>-1</sup> and 1099 cm<sup>-1</sup>, respectively. The absorption band observed at 1741 cm<sup>-1</sup> is due to the carbonyl group of the ester linkage of MMI confirming its incorporation in CO<sub>2</sub>H-PMS. This absorption band of MMI has been observed at similar position when it was grafted to polyethylene chains [37]. The absorption

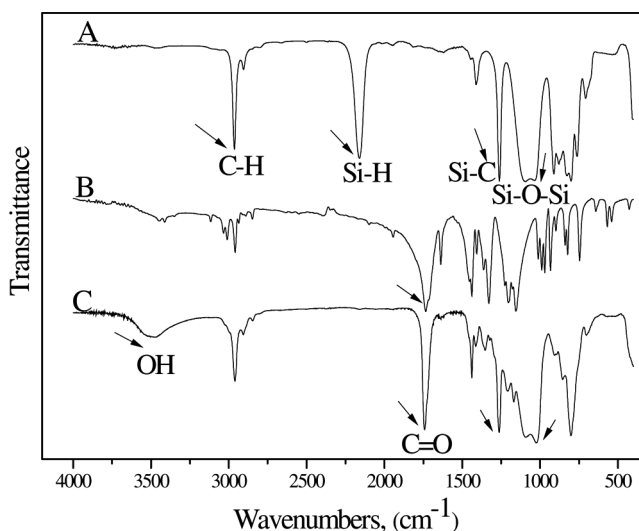


**Figure 3.** FTIR spectra of PDMS-co-PHMS (A), MMI (B) and CO<sub>2</sub>H-PMS (C).

bands at  $1264\text{ cm}^{-1}$  and  $808\text{ cm}^{-1}$  also confirm the presence of the Si-CH<sub>3</sub> bond. On the other hand, the TG analysis showed that CO<sub>2</sub>H-PMS was thermally more stable than the starting PDMS-co-PHMS copolymer. TG results of PDMS-co-PHMS showed a maximum decomposition temperature at 406°C and the synthesized CO<sub>2</sub>H-PMS template shows two stage decomposition at 438°C and 694°C (data not shown).

It is known that CaOx is the main compound of HKS, in which three polymorphs of calcium oxalate monohydrate (COM), calcium oxalate dihydrate (COD) and calcium oxalate trihydrate (COT) has been described [7,38]. Thus, COM is elongated hexagonal crystals with an average size of  $5.0 \times 2.0\text{ }\mu\text{m}$ , where the surfaces of most crystals are rough. In the case of COD bipyramid morphology with eight faces has been described. Atomic force microscopy measurements reveal that the adhesion strength of COM and COD faces, using functional groups *i.e.*, COO<sup>-</sup> and NH<sub>2</sub> as a probe, decrease in the order COM (100) > COD (100) = COM (12 $\bar{1}$ ) > COM (010) > COD (101). This ranking establishes a crucial link between the pathologic behaviors of COM and COD and the adhesion strengths of their respective crystal surfaces, and supports the critical roles of aggregation and crystal adhesion to renal epithelial cells in the HKS formation. COM, the pathogenic form, exhibits large {100} faces when is grown in urine-like media. The kidney stones often contain stacks of COM plates emanating from a central nidus attached to renal surfaces. These stacks are developed by crystal-to-crystal attachment of the large {100} faces. Thus the most prominent COM face exhibits the largest adhesion strength, an ideal combination for creating robust COM aggregates and strong attachments to epithelial cell that can persist under stresses experiencing during flow in the renal tubules. Conversely, the protective COD crystals always exhibit extended {101} faces when grown in urine-like media and the exposed area of COD {100} is minimal. Thus, the more adherent face, COD {100}, is nearly inaccessible for adhesion contacts. Instead, the most prominent face, COD {101}, displays the weakest condition strength. This condition would make COD aggregates and attachments to cell membranes less stable, thereby reducing the tendency to form stones, as reflected by the large amounts of individual COD microcrystals found in voided urine [39].

Macromolecules isolated from urine of healthy people inhibit the crystal growth of COM *in vitro*, favoring the formation of COD over COM. Two reported candidates for inhibition of this crystal formation are Osteopontin (OPN) and Tamm-Horsfall protein (THP). OPN is an acidic phosphorylated glycoprotein isolated from bone matrix, which contains several sequence domains that are rich in the dicarboxylic acid and aspartic acid. It is believed to play a role in modulating mineralization of normal bone by enhancing the osteoclast activity and halting hydroxyapatite crystal growth [40]. OPN is also expressed by normal renal epithelial cells, particularly cells of the ascending limb of Henle's loop and the distal convoluted tubules [41,42]. THP is also expressed by the kidney epithelial cells, but unlike OPN, THP is kidney specific [43,44]. The precise mechanism by which THP and OPN has inhibitory effect on CaOx formation is under investigation, but it appears that direct binding between these macromolecules and Ca<sup>2+</sup> ions or Ca-crystals may be crucial. Both proteins contain Ca-binding motifs, with OPN having one and THP having two in its epidermal growth factor (EGF)-like repeats [42]. Alternatively, THP and OPN could bind to Ca<sup>2+</sup> via their abundant negatively charged groups. THP is highly sialylated, whereas OPN is both sialylated and highly phosphorylated

at its clusters of serine and threonine residues [45,46]. The multiple consequences of this binding reaction are: (a) reducing the intratubular  $\text{Ca}^{2+}$  concentration to below the threshold of crystallization, (b) inhibiting Ca-crystal aggregation and growth, and (c) blocking crystals from adhering to the renal epithelial cells, a critical step in HKS retention [47].

In order to evaluate the effect of carboxylate moieties of  $\text{CO}_2\text{H-PMS}$  as an additive on *in vitro* CaOx mineralization, a set of experiments was performed and the morphology of the resultant CaOx crystals was observed. The CaOx crystallization was carried out at  $25^\circ\text{C}$  and  $37^\circ\text{C}$ , since previous studies have been conducted at these temperatures [48,49]. Mineralization experiment at  $37^\circ\text{C}$ , emulating the physiological conditions, was also performed. Additionally, we tested the effect of PMS and  $\text{CO}_2\text{H-PMS}$  on CaOx crystallization *in vitro* varying the pH values at 4, 6 and 9. Figure 4 shows SEM images of CaOx crystals grown in the presence of PMS and  $\text{CO}_2\text{H-PMS}$  as additive during mineralization assays at  $32\text{ }\mu\text{g/ml}$  and  $1\text{ mg/ml}$  concentrations with pH 4 and 9 at both temperatures. Figure 4A shows the morphology of the  $0.2\text{ }\mu\text{m}$  Millipore filter's surface. Figure 4B shows a grouped flat of contact twin COM crystals with predominance of  $\{100\}$  face with  $13.6 \times 4.95\text{ }\mu\text{m}$  of size when  $32\text{ }\mu\text{g/ml}$  of PMS was present at pH 4 at  $20^\circ\text{C}$ . Similarly flat twin COM morphology with  $32\text{ }\mu\text{g/ml}$  PMS at pH 4 but at  $37^\circ\text{C}$  were observed. Figure 4D show the influence of  $32\text{ }\mu\text{g/ml}$   $\text{CO}_2\text{H-PMS}$  as additive at pH 4 at  $20^\circ\text{C}$ . Here we observed aggregated COM crystals with  $\{010\}$  and  $\{100\}$  faces. The effect of pH can be seen in Figure 4E, where we used  $32\text{ }\mu\text{g/ml}$  of  $\text{CO}_2\text{H-PMS}$  at pH 9 at  $20^\circ\text{C}$ . In this case we observed single and aggregated twin COM crystals with  $\{010\}$  and  $\{100\}$  faces (not observed at this magnification). We also observed single COD crystals with tetragonal bipyramidal shape. Finally, when the  $\text{CO}_2\text{H-PMS}$  was used at  $1\text{ mg/ml}$  concentration in a buffered solution at pH 9 and at  $37^\circ\text{C}$  (Fig. 4F) we observed both COM and COD crystals. Contact twin of COM crystals with  $\{010\}$

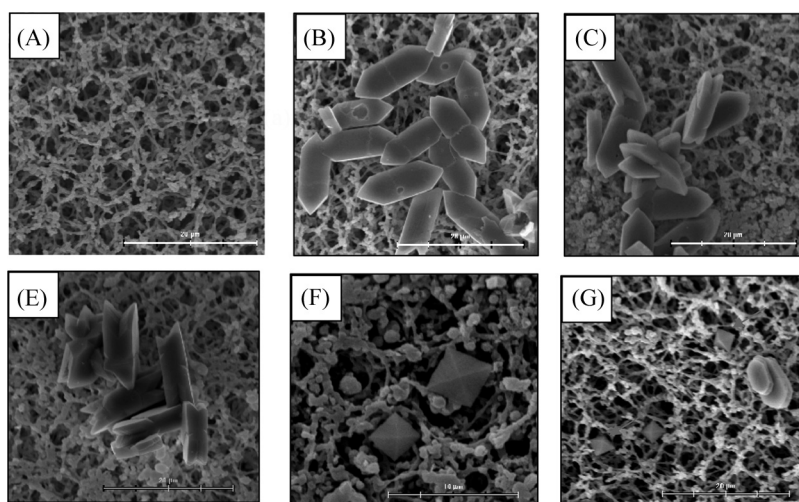


**Figure 4.** SEM images of Millipore filter (A), and CaOx crystals formed in presence of  $32\text{ }\mu\text{g/ml}$  PMS at pH 4 and at  $20^\circ\text{C}$  (B),  $32\text{ }\mu\text{g/ml}$  PMS at pH 4 and at  $37^\circ\text{C}$  (C),  $32\text{ }\mu\text{g/ml}$   $\text{CO}_2\text{H-PMS}$  at pH 4 and at  $20^\circ\text{C}$  (D),  $32\text{ }\mu\text{g/ml}$   $\text{CO}_2\text{H-PMS}$  at pH 9 and at  $20^\circ\text{C}$  (E) and  $1\text{ mg/ml}$   $\text{CO}_2\text{H-PMS}$  at pH 9 and at  $37^\circ\text{C}$  (F).

and {100} faces are observed. Moreover, single COD crystals with tetragonal bipyramidal shape and {011} face were observed.

We found that both concentrations of CO<sub>2</sub>H-PMS were able to modify the nucleation and crystal growth of CaOx. Moreover, the stabilization of COD and its dissolution and re-crystallization process in COM was avoided. The COD crystals were observed at pH 9 when CO<sub>2</sub>H-PMS was used at 32 µg/ml and 1 mg/ml at 20°C and 37°C, respectively (Fig. 4E and F). These observations are in agreement with previous studies, where anionic macromolecules could inhibit the nucleation, growth and aggregation of CaOx crystals, and are involved in the *in vitro* cells attachment [50,51].

On the other hand, it is known that PMS has a much higher permeability to gases than other synthetic polymers, which can be convenient for the current gas diffusion set up. This occurs because of the torsion and bending flexibility of CO<sub>2</sub>H-PMS as an organosiloxane compound, which elicits a characteristic nucleation and growth of CaOx crystals. We suspect that the CO<sub>2</sub>H-PMS is adsorbed on the CaOx surface. Consequently, the carboxylate groups could induce a local Ca<sup>2+</sup> ion accumulation. This is more pronounced at higher pH acting as nucleation sites thereby leading to the formation of CaOx crystals by heterogeneous crystallization. The presence of Si atoms on the surface of CaOx crystals by SEM-EDS is under study.

Anionic bioorganic molecules extracted from *Semen Plantaginis* and *Folium Pyrrosiae* can induce crystal growth of CaOx with similar mechanism [52]. Silica (SiO<sub>2</sub>) molecules, for example, decrease the size of COM crystals and promote the formation of COT in detriment of COM [53]. This may be explained by specific geometric relationship between active functional groups of SiO<sub>2</sub> e.g., surface hydroxyl groups and interatomic distances on the crystal faces of COT. Thus, attachment of newly formed crystals to renal epithelial cells appears to be a critical step in the development of HKS, but only preliminary information is available about the molecules mediating this interaction [54–56]. Pre-coating of COM crystals with polyanions and pre-coating of cells with polycations inhibited crystal attachment to cultured renal epithelial cells [57,58], implying that anionic cell surface molecules play a prominent role in attachment of crystals to the cells. Crystal adhesion decreased markedly after neuraminidase and trypsin treatment of BSC-1 cells, suggesting that the role of anionic sialic acid-containing proteins in the binding process is crucial [59]. Thus, annexin II (Ax-II) proteins has been identified as potential crystal-binding molecules on the apical surface of MDCKI cells [60]. These molecules have been characterized as a conserved COOH-terminal protein that mediates their membrane and Ca-binding properties. COM crystal adhesion decreased significantly after MDCKI cells were pretreated with a monoclonal antibody against Ax-II. However, crystal binding to antibody-treated cells was not abolished completely, suggesting that Ax-II may be one of several cell surface crystal-binding molecules e.g., glycoprotein, phospholipid, GAGs, etc. Therefore, in the intact nephron Ax-II could mediate adhesion of COM crystals to cells allowing endocytosis, and altered exposure of Ax-II on the surface of injured renal tubular cells could promote crystal retention and possibly HKS formation. Apoptosis is another mechanism involved in crystal attachment to epithelial cells following injury. Apoptotic changes include exposure of annexin binding phosphatidylserine to the cell surface as well as morphological changes [61–63]. Negatively charged phosphatidylserine attract Ca<sup>2+</sup> and can act as sites for the attachment of calcific crystals to the cell surfaces [64]. The supersaturation of urine by Ca<sup>2+</sup> and oxalate ions is not the only factor to explain

the urolithiasis. Another important factor is that in renal epithelial cells hyperoxaluria increases generation of free radicals, including  $O_2^-$ , hydroxyl radical ( $OH\bullet$ ), hydrogen peroxide ( $H_2O_2$ ), peroxide radical ( $RO\bullet$ ) and singlet molecular oxygen [65]. These changes are predisposing factors for the facilitation of crystal adherence and retention [66–71]. Recently, it has been reported that extracts obtained from the plants *Quercus salicina* Blume and *Quercus stenophylla* Makino (QS extracts) prevented renal injury induced by exposure to oxalate for 24 h in a dose-dependent manner suppressing the increase in NADPH-induced  $O_2$  production, or NADPH oxidase activity [72]. Antioxidant activity such as SOD, catalase and vitamin E suppress the release of LDH and the formation of malondialdehyde in LLC-PK<sub>1</sub> and MDCK cells indicating that the protective action of QS extract against oxalate-induced cell injury may be attributed to its radical scavenging effects.

## Conclusion

We have demonstrated that by using CO<sub>2</sub>H-PMS as template, we can effectively control the morphogenesis and the crystallographic polymorphism of CaOx crystals. The composition and concentration of this template as additive, pH and temperature of mineralization solution seem to be crucial during CaOx nucleation and growth. At different pH, the carboxylate groups of CO<sub>2</sub>H-PMS can undergo different degree of dissociation resulting in different polymer conformation in solution that could affect CaOx morphology. The crystallization of CaOx triggered by the presence of CO<sub>2</sub>H-PMS, results from a local accumulation of  $Ca^{2+}$  ions, which correlates closely with the pH of the mineralization solution. FTIR analysis is in good agreement with the proposed PMS structures. SEM analysis showed contact twin COM crystals when crystal grew in presence of PMS and tetragonal bipyramidal COD crystals when CO<sub>2</sub>H-PMS was used. By using this new template, we were able to stabilize the COD crystal and its dissolution-recrystallization process in COM was avoided. COD crystals were observed at pH 9 when CO<sub>2</sub>H-PMS was used at 32 µg/ml and 1 mg/ml at 20°C and 37°C, respectively. SEM-EDS and XRD studies of CaOx crystals are under progress. In summary, the use of PMS and its derivative as templates provides a viable approach for studying various aspects of biomineralization including production of controlled polymorphs and defined CaOx morphologies.

## Acknowledgments

This research was supported by FONDECYT 11070136 and FONDAP 11980002 granted by the Chilean Council for Science and Technology (CONICYT).

## References

- [1] Bihl, G. & Meyers, A. (2001). *Lancet.*, 358, 651.
- [2] Barbas, C., Garcia, A., Saavedra, L., & Muros, M. (2002). *J. Chromatogr. B Analyt. Technol. Biomed. Life Sci.*, 781, 433.
- [3] Lieske, J. C., Leonard, R., Swift, H. S., & Toback, F. G. (1995). *Am. J. Physiol.*, 270, F192–F199.
- [4] Hess, B., Zipperle, L., & Jaeger, P. (1993). *Am. J. Physiol.*, 265, F784.
- [5] Coe, F. L. & Parks, J. H. (1988). *Physical chemistry of calcium stone disease*, Year Book Medical: Chicago, p. 38.

- [6] Wahl, C. & Hess, A. (2000). *Ther. Umsch.*, 57, 138.
- [7] Millan, A. (2001). *Cryst. Growth Des.*, 1, 245.
- [8] Holmes, R. P., Goodman, H. O., & Assimios, D. G. (2001). *Kidney Int.*, 59, 270.
- [9] Benitez, I. O. & Talham, D. R. (2004). *Langmuir*, 20, 8287.
- [10] Benitez, I. O. & Talham, D. R. (2005). *J. Am. Chem. Soc.*, 127, 2814.
- [11] Khan, S. R., Whalen, P. O., & Glenton, P. A. (1994). *J. Cryst. Growth*, 135, 523.
- [12] Brown, C. M., Novin, F., & Purich, D. L. (1994). *J. Cryst. Growth*, 135, 523.
- [13] Wu, X., Ouyang, J., Deng, S., & Cen, Y. (2006). *Chinese Chem. Lett.*, 17, 97.
- [14] Brook, M. A. (2000). *Silicon in organic, organometallic, and polymer chemistry*, John Wiley & Sons INC.: USA.
- [15] Abe, Y. & Gunji, T. (2004). *Prog. Polym. Sci.*, 29, 149.
- [16] Jones, R. G., et al. (2000). *Silicon-containing polymers*, Kluwer Academic Publishers: Dordrecht.
- [17] Martciniec, B., Gulinski, J., & Maciejewski, H. (2000). In: *Encyclopedia of catalysis, hydrosilylation*, Horvath, I. T. (Ed.), Vol. 4, Wiley, New York, p. 107.
- [18] Hu, S., Ren, X., Bachman, M., Sims, C. E., Li, G. P., & Allbritton, N. L. (2004). *Langmuir*, 20, 5569.
- [19] Sia, S. K. & Whitesides, G. M. (2003). *Electrophoresis*, 24, 3563.
- [20] Wegner, G. (2000). *Acta Mater.*, 48, 253.
- [21] Liu, M., et al. (2003). *Biomedical applications of polymer colloids*, Elaïssari, Abdelhamid (Ed.) Mercel Dekker Inc., p. 747.
- [22] Kaneko, Y., Sato, S., Kadokawa, J.-I., & Iyi, N. J. (2006). *J. Mater. Chem.*, 16, 1746.
- [23] Lee, S. & Vörös, J. (2005). *Langmuir*, 21, 11957.
- [24] Zhang, X. D., Macosko, C. W., Davis, H. T., Nikolov, A. D., & Wasan, D. T. (1999). *J. Colloid. Interf. Sci.*, 215, 270.
- [25] Ojima, I. (1989). *The hydrosilylation reaction: The chemistry of organic silicon compounds*, Patai, S., et al. (Eds.), p. 1479.
- [26] Speier, L. J. (1979). *Homogeneous catalysis of hydrosilation by transition metals*, Adv. Org. Chem., Vol. 17, Academic Press: USA.
- [27] Grassmann, O. & Lobmann, P. (2004). *Biomaterials*, 25, 277.
- [28] Arias, J. L., Neira-Carrillo, A., Arias, J. I., Escobar, C., Boderó, M., David, M., & Fernandez, M. S. (2004). *J. Mater. Chem.*, 14, 2154.
- [29] Neira-Carrillo, A., Pai, R. K., Fernández, M. S., Carreño, E., Vasquez-Quitral, P., & Arias, J. L. (2009). *Colloid. Polym. Sci.*, 287, 385.
- [30] Neira-Carrillo, A. PhD Thesis. (2003). *Síntesis vía Catiónica de Derivados de Polisiloxanos-Polisilazanos – Precursores de Materiales Cerámicos y de Agentes de Dispersión y Mineralización*. University of Concepción.
- [31] Yazdani-Pedram, M., Vega, H., & Quijada, R. (2001). *Polymer*, 42, 4751.
- [32] Apfel, M. A., Finkelmann, H., Janini, G. M., Laub, R. J., Lühmann, B.-H., Price, A., Roberts, W. L., Shaw, T. J., & Smith, C. A. (1985). *Anal. Chem.*, 57, 651.
- [33] Neira-Carrillo, A., Pai, R. K., Fuenzalida, V. M., Fernández, M. S., Retuert, J., & Arias, J. L. (2008). *J. Chil. Chem. Soc.*, 53, 1469.
- [34] Yamaguchi, S., Yoshioka, T., Utsunomiya, M., Koide, T., Osafune, M., & Okuyama, A. (1993). *Urol. Res.*, 21, 187.
- [35] Pouchert, J. C. (1975). *The aldrich library of infrared spectra*, Aldrich Chemical Co. Inc.: USA.
- [36] Rodríguez-Baeza, M., Neira-Carrillo, A., & Aguilera, J. C. (2003). *J. Chil. Chem. Soc.*, 48, 72.
- [37] Lopez-Machado, M. A., Yazdani-Pedram, M., Retuert, J., & Quijada, R. (2003). *J. App. Pol. Sci.*, 89, 2239.
- [38] Monje, P. & Baran, E. (2002). *Plant Physiol.*, 128, 707.
- [39] Sheng, X., Ward, M. D., & Wesson, J. A. (2005). *J. Am. Soc. Nephrol.*, 16, 1904.
- [40] Giachelli, C. M. & Steiz, S. (2000). *Matrix Biol.*, 19, 615.

- [41] Min, W., Shiraga, H., & Chalko, C. (1998). *Kidney Int.*, 53, 189.
- [42] Mazzali, M., Kipari, T., Ophascharoensuk, V., Wesson, J. A., Johnson, R., & Hughes, J. (2002). *Q. J. Med.*, 95, 3.
- [43] Kumar, S. & Muchmore, A. (1990). *Kidney Int.*, 37, 1395.
- [44] Serafini-Cessi, F., Malagolini, N., & Cavallone, D. (2003). *Am. J. Kidney Dis.*, 42, 658.
- [45] Van Rooijen, J. J., Voskamp, A. F., Kamerling, J. P., & Vliegenthart, J. F. (1999). *Glycobiology*, 9, 21.
- [46] Singh, K., DeVougue, M. W., & Mukherjee, B. B. (1990). *J. Biol. Chem.*, 265, 18696.
- [47] Asselman, M. & Verkoelen, C. F. (2002). *Curr. Opin. Urol.*, 12, 271.
- [48] Escobar, C., Neira-Carrillo, A., Fernandez, M. S., & Arias, J. L. (2007). Role of sulfated macromolecules in urinary stone formation. In: *Biomineralization, from Paleontology to Materials Science*, Arias, J. L., Fernandez, M. S. (Eds.), Editorial Universitaria: Santiago, Chile, p. 343.
- [49] Kramer, G., Steiner, G. E., Prinz-Kashani, M., Bursa, B., & Marberger, M. (2003). *B. J. U. International*, 91, 554.
- [50] Lieske, J. C. & Toback, F. G. (2000). *Curr. Opin. Nephrol. Hypertens.*, 9, 349.
- [51] Jesson, J. A. & Ward, M. D. (2007). *Elements*, 3, 415.
- [52] Zhang, Y., Tao, J., Feng, N., & Han, X. (2008). *Cryst. Res. Technol.*, 43, 931.
- [53] Yu, H., Sheikholeslami, R., & Doherty, W. O. (2004). *J. Cryst. Growth*, 265, 592.
- [54] Riese, R. J., Mandel, N. S., Wiessner, J. H., Mandel, G. S., & Becker, C. G. (1992). *Am. J. Physiol.*, 262, F177.
- [55] Verkoelen, C. F., Van Der Boom, B. G., & Romijn, J. C. (2000). *Kidney Int.*, 58, 1045.
- [56] Kleinman, J. G. & Sorokina, E. A. (1999). *J. Biol. Chem.*, 274, 27941.
- [57] Lieske, J. C., Leonard, R., & Toback, F. G. (1995). *Am. J. Physiol.*, 268, F604.
- [58] Lieske, J. C., Leonard, R., Swift, H. S., & Toback, F. G. (1996). *Am. J. Physiol.*, 270, F192.
- [59] Verkoelen, C. F., Van der Boom, B. G., Kok, D. J., & Romijn, J. C. (2000). *Kidney Int.*, 57, 1072.
- [60] Kumar, V., Farrel, G., Deganello, S., & Lieske, J. C. (2003). *J. Am. Soc. Nephrol.*, 14, 289.
- [61] Kim, J., Cha, J., Tisher, T. C., & Madsen, K. M. (1996). *Am. J. Physiol.*, 270, F535.
- [62] Lieberthal, W., Triaca, V., & Levine, J. S. (1996). *Am. J. Physiol.*, 270, F700.
- [63] Lieberthal, W. & Levine, J. S. (1996). *Am. J. Physiol.*, 271, F477.
- [64] Bigelow, M. W., Wiessner, J. H., Kleinman, J. G., & Mandel, N. S. (1996). *J. Urol.*, 155, 1094.
- [65] Sarica, K., Yagci, F., Bakir, K., Erbagci, A., Erturhan, S., & Ucak, R. (2001). *Urol. Res.*, 29, 34.
- [66] Selvam, R. (2002). *Urol. Res.*, 30, 35.
- [67] Wiessner, J. H., Hasegawa, A. T., & Hung, L. Y. (2001). *Kidney Int.*, 59, 637.
- [68] Khan, S. (1995). *Urol. Res.*, 23, 71.
- [69] Rashed, T., Menon, M., & Thamilselvan, S. (2004). *Am. J. Nephrol.*, 24, 557.
- [70] Thamilselvan, S., Byer, K. J., Hackett, R. L., & Khan, S. R. (2000). *J. Urol.*, 164, 224.
- [71] Thamilselvan, S., Khan, S., & Menon, M. (2003). *Urol. Res.*, 31, 3.
- [72] Moriyama, M. T., Miyazawa, K., Noda, K., Oka, M., Tanaka, M., & Suzuki, K. (2007). *Urol. Res.*, 35, 295.